

# Solid Rocket Motor Thrust Oscillation with Inhibitors due to Vortex Shedding

D. Hyland

*University of Minnesota, Minneapolis, MN 23423*

B. Jackson

*Milwaukee School of Engineering, Milwaukee, WI 53202*

B. Keller

*Virginia Polytechnic Institute and State University, Blacksburg, VA 24060*

*and*

A. Paxson

*University of Alaska Fairbanks, Fairbanks, AK 99775*

*2010 NASA Propulsion Academy, ER-52, MSFC, Huntsville, Al 35812*

**The problem of identifying and attributing vortex shedding to certain causes (inhibitors, propellant cavities, etc) has been a long debated topic in the scientific community. Pressure oscillations within the motor are of increasing concern as it has been discovered that for certain motors the frequency of oscillation is nearing the harmonic frequency of the motor's structure and in some cases the human body. Thrust oscillations can result in guidance and thrust vector control complications and in worst case scenarios these oscillations can result in motor structural failures or severe bodily harm to astronauts. The decision was made to use schlieren photography to view vortex shedding over various inhibitors, through a simulated section of a motor, to develop a relationship between inhibitor size, shape, and placement with pressure oscillations. Although no correlation could be determined, the concept for this experiment lays the groundwork for future research that will help increase the efficiency of the motor, eliminate vortex shedding, and move the aerospace community forward.**

## I. Introduction

Thrust oscillations have been a source of debate and concern over the last 50 years during the development of solid rocket motors. When these oscillations match the motors inherent oscillation modes the amplitude of these oscillations increases drastically. In the case of the Space Shuttle Reusable Solid Rocket Motor (RSRM) a one psi pressure oscillation results in a 33,000 lbf thrust oscillation which results in large vibration loads on both the shuttle's payload and crew.<sup>1</sup> In the case for the Ares I, thrust oscillations were identified as a major risk to the Ares project and were assigned a four by five on NASA's risk matrix.<sup>2</sup> Several methods have been proposed to prevent the oscillations from affecting the crew and payload; however, most methods attempt to dampen the effects rather than then prevent the occurrence of the oscillations. This experiment set out to determine a correlation between pressure oscillations and the vortices generated by combustion gases flowing over the inhibitors. A thrust trace and frequency plot for a simulated motor are shown in Fig 1a and 1b, respectively.

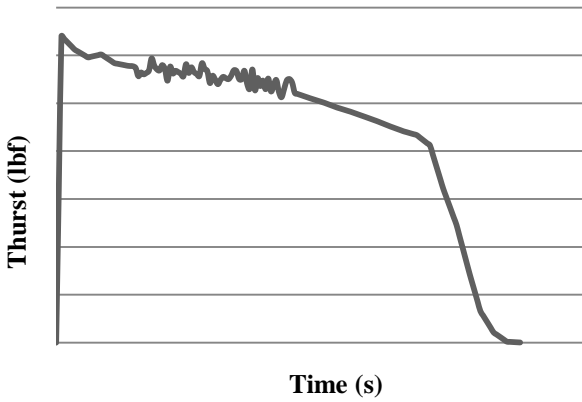


**Figure 1a: Thrust vs. Time Plot for Simulated SRM**

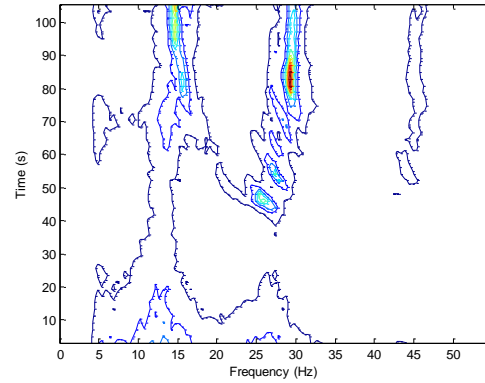


**Figure 1b: Frequency vs. Time Plot for Solid Rocket Motor**

Multiple studies have been conducted and many models, utilizing both CFD programs as well as other forms of empirical mathematical modeling, have been developed. The Flandro Model was based on the assumption that instead of instability due to combustion, shock waves are the dominant source of nonlinear losses.<sup>3</sup> In a paper written specifically relating to the Solid Rocket Motor Upgrade (SRMU), a motor without inhibitors designed for the Titan IV, the acoustic feedback model was examined by K.W. Dotson et al, trying to explain how a vortex moves through a SRM. The theories presented show that the length of vortices (regardless of their source) are not of constant length (increases with distance from origin) and that nearby vortices can combine to form a larger single vortex. Using PV-Ware (empirical) to solve equations and then running the results through NASTRAN and an FFT, D.R. Mason et al, were able to show that indeed the highest amplitude pressure oscillations occurred on the acoustic modes (1L, 2L, 3L, etc) the first number being their harmonic number. Using CFD, it was shown how the vortices progressed through the ETM-3 and the Shuttle RSRM motors. With the use of weak parameters the simulated data matched field data; however, it contained a significant amount of error. This led to the firm definition of three known sources of vortices; wall layer interaction, inhibitor interaction, and flow over propellant cavities.<sup>4</sup> An example of the vortex shedding phenomena is shown below in Fig. 2.

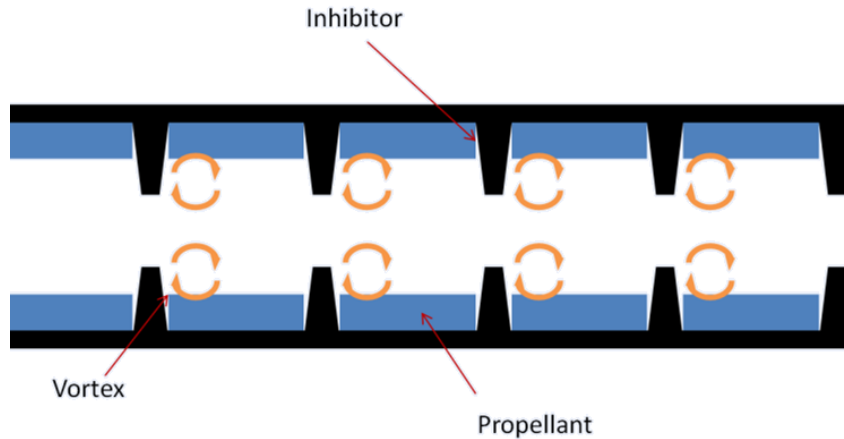


**Figure 2: Simulated Vortex Shedding in a Solid Rocket Motor**

## II. Background

Although schlieren photography has been around since the 17<sup>th</sup> century, the 19<sup>th</sup> and 20<sup>th</sup> centuries brought about its aerospace applications. The applications of schlieren in wind tunnels include visualizing subsonic and supersonic flows, examining turbulent flows over vehicles, and a basis the beginning of computational fluid dynamics. However, schlieren photography is only available in 2-D and it is not in true color. Despite these disadvantages this technology can be utilized to view vortices in a modeled SRM cavity.

Schlieren photography and shadowgrams utilize a phenomenon where light passing through materials of different density, thus different refractive indices, is refracted. The angle of refraction is directly related to the refractive index of the medium. For both setups both mirrors and lenses can be used to obtain results, however as a result of chromatic aberrations resulting from light passing through the glass of a lens, mirrors are often preferred. Despite being closely related, shadowgraphs vary from schlieren in two distinct ways. Shadowgrams are not focused images, but a shadow of the object being observed. Schlieren systems use a series of optics to focus the image to obtain a precise representation of the object of interest. Second, schlieren setups require a knife-edge or filter to cut off refracted light rays. The resulting image from this method is more sensitive than the one obtained from a shadowgram. Shadowgram and schlieren arrangements are shown in Fig. 3 and 4, respectively. In interest of higher sensitivity a schlieren arrangement was chosen for this experiment.

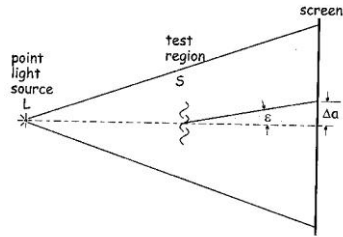


**Figure 3: Early Shadowgraph Setup**

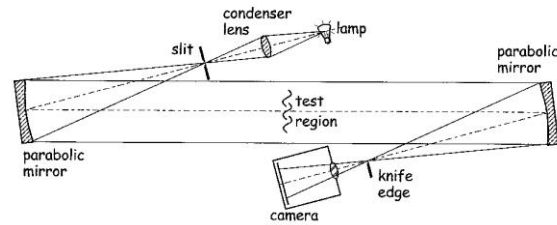


**Figure 4: Z-Schlieren Setup with Razor Blade Cutoff**

The knife-edge cut off characteristic of schlieren photography is shown in Fig. 4. Light diffracted by the field of interest will not be parallel with the non-diffracted light; therefore, it will not condense to the same point after being reflected by the second mirror. By placing a cut-off at the focal point of the second mirror the diffracted rays will be removed, resulting in a more sensitive image. Typically a razor blade is used as a cutoff, which can either be oriented vertically or horizontally. It was determined that by positioning the blade horizontally a more detailed image was obtainable for our setup. The process by which the knife-edge removes diffracted rays is shown in Fig. 5.

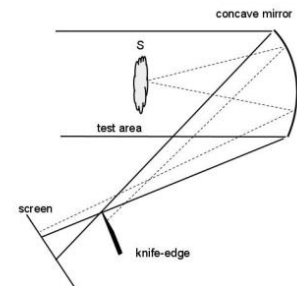


**Figure 5: Knife-Edge Cut-Off**

### III. Methodology

To achieve the objective of this experiment, three milestones were initially identified as:

- 1) Visualize vortex-shedding resulting from inhibitors using schlieren photography
- 2) Correlate video of vortex-shedding with pressure frequency traces
- 3) Determine a relationship between various heights and placement of inhibitors and their affect on vortex formation

The following details the development of several tools necessary to accomplish these milestones.

#### A. Schlieren Setup

In order to obtain a point source of light, a 12-volt automotive head lamp was used. This type of bulb was selected since it contained a short straight filament which could be approximated as a point source. The bulb was placed inside a metallic electrical box which had a hole drilled in the front. An adjustable diameter iris was placed over this hole which was located directly in front of the bulb. A variable voltage DC power supply was used in attempt to supply a constant current to the lamp. Adjustable optics stands and towers were used to create a permanent set up and were used to adjust the positioning of the optics and light source to obtain a precise image. Fig. 6 displays the experimental set up used.

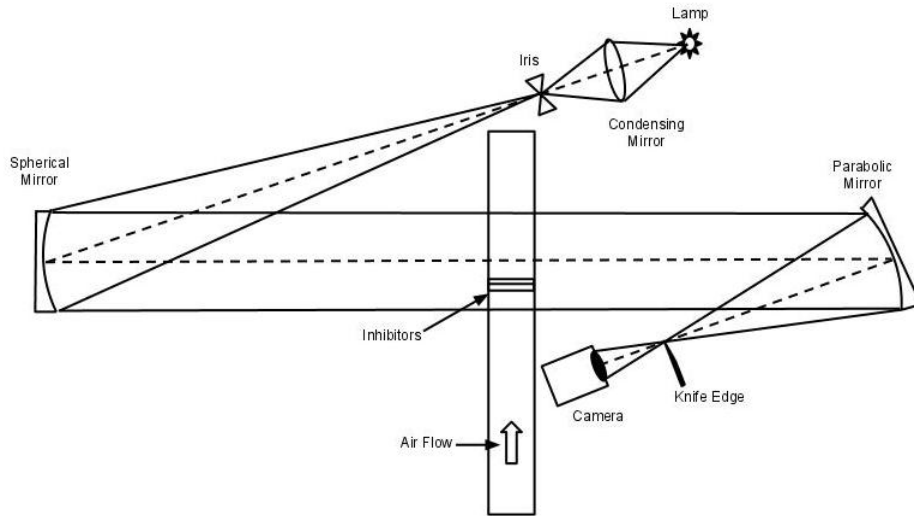


**Figure 6: Experimental Setup Diagram**

Two different types of mirrors were used (one spherical, one parabolic) due to spatial constraints of the optics table. Parabolic mirrors are generally preferred for use in schlieren photography because they are ideal for focusing parallel light rays to an exact point and creating parallel rays from a point source. However, since the focal ratio for the spherical mirror was greater than 10, the errors resulting from this mirror are negligible. The focal lengths of the spherical and parabolic mirrors used are 50-in and 18-in, respectively. The spherical mirror was incorporated for reflecting the light source first since the large focal point collimates the light better due to its increased length. The parabolic mirror was added so that its small focal point allowed it to receive the light and bring it to a point so the camera and razor could fit between it and the test chamber. This allowed the entire test arrangement to fit within the limits of the optics table (8X4 feet). A picture displaying this setup is shown below in Fig. 7:

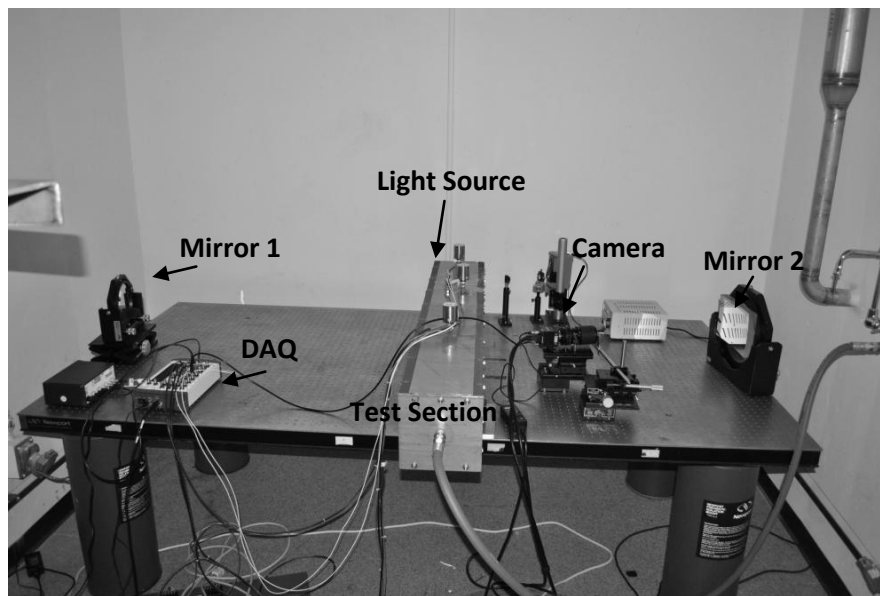


**Figure 7: Experimental Setup**

The z-type arrangement chosen for this experiment results in off-axis aberrations called coma and astigmatism. Coma occurs when the point source of light is off axis of the mirror. The light source is intentionally off axis of the mirror such that it will not be in the field of interest. However, the resulting light rays refracted by the mirror will not be perfectly parallel. Likewise when light contacts the second mirror the rays will not be perfectly focused to a

point, resulting from the second mirror being positioned to focus light off axis as well. An astigmatism results since the distance from the point source to the mirror is not constant for any point on the mirrors surface. This aberration can be minimized by using selecting large f-value mirrors and minimizing the angle of offset angle. However, the extent that the angle of offset could be reduced was limited by the position of the test chamber on the table. As a result the angle of offset was larger than desired. For future experiments the alignment of the optics with respect to the test chamber should be taken into greater consideration.

## B. Test Chamber

To simulate on a small scale the inner workings of a SRM, a rectangular test section was designed. The test section consisted of a top and bottom constructed of aluminum, and two clear acrylic sides. Aluminum inhibitors were placed inside the test section to act as flow-tripping devices. A nozzle was simulated using a fixed steel plate on the aft end shown in Fig. 8.a. Compressed air at 125 psig is flown through the inlet of the SRM mock assembly where the schlieren photographs are taken. The cold flow enters in a custom inlet (shown in Fig. 8) which was designed to spread the flow the full cross sectional area of the test apparatus such that it would be fully expanded before contacting the mock inhibitor. To diffuse the inflowing air a porous polyethylene tube was placed over inlet hole. The complete test chamber is shown in Fig. 9.

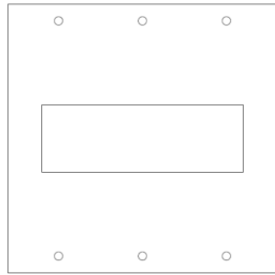


Figure 8.a: Test Section Nozzle

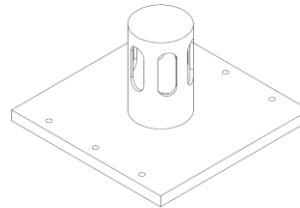


Figure 8.b: Cold Flow Inlet

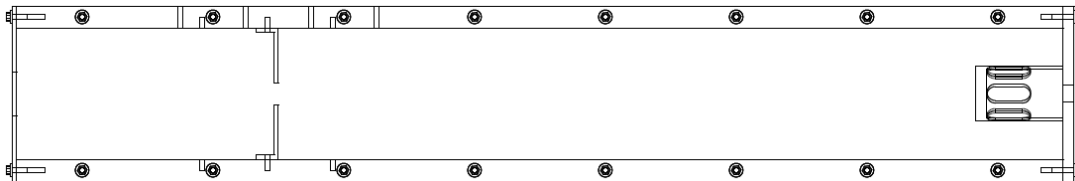


Figure 9: Test Section

## C. Pressure Measurements

To obtain pressure data, four pressure transducers and two dynamic pressure transducers, or microphones, were utilized. Pressure transducers were placed half-way between the inlet and the inhibitor, before and after the top inhibitor, and before the nozzle. The microphones were placed before and after the inhibitor located on the top of the chamber.

The LABVIEW code used to record and write pressure data was modified from an existing block diagram generated for a similar cold flow experiment. Modifications were made to the code so that a trigger would be sent to the high speed camera so the recording of the camera and pressure sensors would begin simultaneously. Data was initially collected at a frequency of 1,000 Hz, allowing frequencies to be calculated up to 500 Hz using FFTs. MATLAB was utilized for data analysis of the dynamic pressure sensors. The code written was designed to perform two forms of analysis. The first form was a 2-D frequency plot across the entire time range. This plot gave an overview of all of the frequencies present in the sample. The second analysis was a time-based one-sided FFT designed to show any variations in frequency with respect to time. To perform this analysis, the sample data was separated into 30 equal time divisions. An FFT was performed on each of these divisions and the resulting frequencies were correlated with the average time for the sample. These calculations are presented as both a 3D waterfall and a contour plot. These graphical methods were chosen to allow for an easy visual analysis to determine any change in the frequency spectrum over a given time span.

## IV. Results

### A. Schlieren Results

This experiment proved that the airflow across the inhibitor can be illustrated by the schlieren apparatus. The vortex shedding across the inhibitor was not clearly visible primarily due to the low pressure of the test chamber, which created small, diffused vortices. These vortices had a small curve in their movement, but did not have a dedicated spiral in their path as expected. The turbulence was displayed by a MATLAB program, which removed the background image, leaving only the moving air in the visual frame. Regardless, the schlieren photography was sensitive enough to see the heat coming off a hand, and was able to produce several clear images of heat from a match and soldering iron.

Additionally, the 125 psig hose allowed direct image capture of supersonic flow containing mach diamonds. This proved that the schlieren apparatus itself was not primarily to blame for the difficulty in visualizing vortex shedding but rather the test chamber. The reasoning for this statement is that several different tests were run using the apparatus and all clearly illustrated the density change of the air. A clear image of a soldering iron's heat was seen through the glass and so the image was not distorted enough through the acrylic to be a concern. Thus, the only remaining factor was the apparatus in which its airflow was not sufficient to create a stable vortex generation. Photographs taken to demonstrate the functionality of the schlieren system are shown in Fig. 10a and 10b:

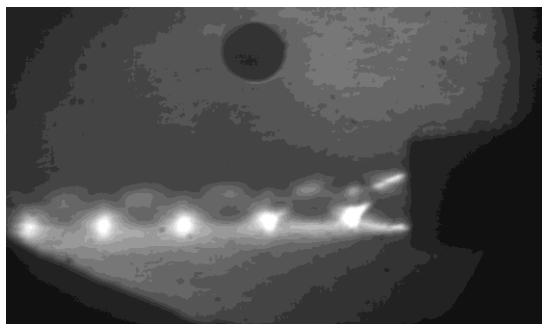


Figure 10a: Air Jet From Low Pressure Inlet

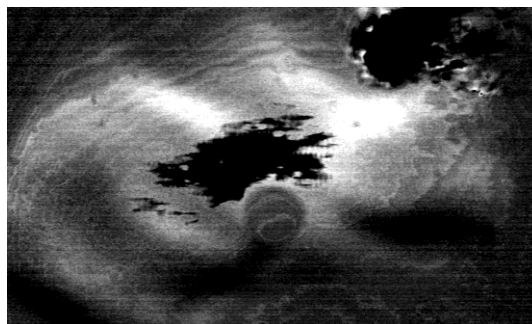
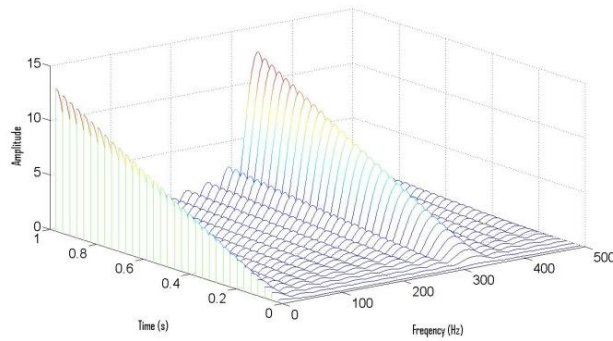


Figure 10b: Vortex Shedding

### B. Pressure Results

The acquisition of pressure data was faced with several technical problems throughout the duration of cold flow experimentation. Initially, the signal conditioner which was connected between the microphones and the DAQ system was one source of complication. It was noticed that the voltage being received from the generator was exponentially declining after first being turned on. Through referencing technical support it was determined that this decline was a result of the capacitance in the signal conditioner – microphone circuit. After experimentally determining the time constant (20 seconds), it was decided to allow five time constants, to pass to allow the signal to reach steady state, prior to the acquisition of data.

After processing the first batch of pressure data through the MATLAB script it was discovered that all samples contained white noise across the entire frequency spectrum with a spike at approximately 0 Hz and 340 Hz. These results for one sample are shown in Fig. 11a and 11b:



**Figure 11a: Waterfall Plot of Frequency Spectrum**

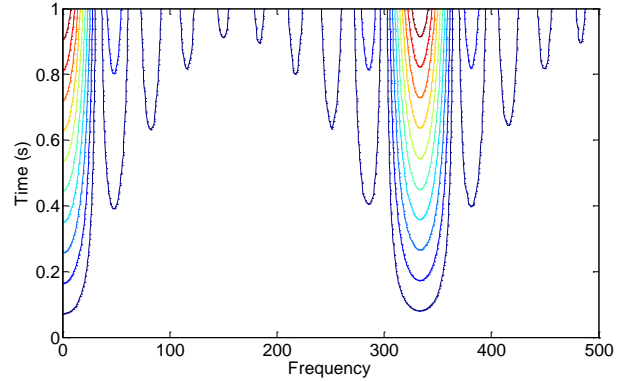


**Figure 11b: Contour Frequency Plot**

Based on expected results, an error in the analysis was immediately suspected. An attempt was made to determine if the error was a result of the algorithm used by MATLAB in the FFT calculations. Several sample sets of data were generated which incorporated various frequencies sampled at 1,000 Hz. These sets were analyzed with the software and yielded expected results. Based on these results the error was identified as originating prior to the FFT analysis. Additional samples of data were collected at a frequency of 10,000 Hz, which likewise yielded similar results to the first sample set. Finally, to determine whether the microphones were functioning properly a speaker was placed inside the test chamber which produced a tone at a constant frequency. The resulting FFT analysis showed a spike at that frequency, proving that the microphones were operating properly.

Based on the experiments proving the proper operation of the microphones, DAQ system, and MATLAB code, it was determined that the lack of a distinguished frequency was a result of the test chamber not oscillating at any set frequency.

## V. Conclusion

The concept of using Schlieren photography is a viable option to visualize vortex shedding off of inhibitors. If more time were available, further progress could have been made to find a direct correlation between vortex generation rates and pressure oscillations. With this correlation developed, research in different inhibitor shapes, sizes, and locations could be tested to discover their impact on vortex shedding which could potentially reduce these pressure oscillations drastically. A few improvements to the design could include:

### A. Test Chamber Improvements

As testing progressed and air flow was visualized through the test apparatus, several faults in the experimental design were discovered. As flow tripped over the inhibitor, it was apparent that the air was not completely laminar when reaching the inhibitors. It was determined that a narrower, longer test chamber would have allowed the air to fully expand, and serve the needs of the experiment better. This would lead to a complete redesign of the test apparatus, but not the schlieren photography arrangement. The problems with the flow were attributed to several other factors that would need to be addressed in a redesign. In a wind tunnel, flow is straightened twice, once horizontally (accomplished using the porous polyurethane wall material) and longitudinally usually with some type of honeycomb structure or screen. These types of structures would establish laminar flow within the test chamber. The same material from the inlet could be used as a screen to help stabilize the flow. To observe the vortices, a higher mass flow is needed. A greater mass flow rate can be achieved either by increasing the inlet pressure, or by decreasing the cross sectional area of the test chamber. These are all ideas that should be adequately addressed should experiments of this kind continue.

### B. Schlieren Improvements

Improvements on the schlieren apparatus would be to incorporate two similarly shaped mirrors (as opposed to the current spherical/parabolic arrangement) so that the light reflected is not bent unusually. To accomplish this, larger mirrors with greater focal lengths would be desired which would require a larger test facility. This would

create improved collimation of light resulting in less distortion. It was also observed that the intensity of the point source was oscillating when high frame rates were used. This is a result of the power source used in the experiment not receiving constant current. A battery used as a replacement would allow the current to be constant enough to generate a steady light.

### **Acknowledgments**

This research work was performed under the NASA Propulsion Academy Program sponsored by Marshall Space Flight Center, Alabama Space Grant Consortium, and the space grants of our respective states. Additionally, special thanks would like to be given to our PI's Philip Franklin of ER-52, Jonathan Jones of ER-51, Tony Marshall of Jacobs Engineering, and Stephen F. Cash for funding the equipment necessary to conduct this research.

### **References**

---

<sup>1</sup> Blomshield, F.S., "Historical Perspective of Combustion Instability in Motors: Case Studies," AIAA Paper 2001-3875, July 2001, pp 1-13.

<sup>2</sup> Cowing, K., "NASA's Exploration Systems Mission Directorate Responds to Ares 1" SpaceRef January 2008, [<http://www.spaceref.com/news/viewnews.html?id=1266>. Accessed 8/1/10.]

<sup>3</sup> Flandro, G.A., "Approximate Analysis of Nonlinear Instability with Shock Waves," AIAA Paper 82-1220, June 1982.

<sup>4</sup> Mason, D.R., Morstadt, R.A., Cannon, S.M., Gross, E.G., Nielson, D.B., "Pressure Oscillations and Structural Vibrations in Space Shuttle RSRM and ETM-3 Motors," AIAA Paper 2004-3898, July 2004, pp 1-17.

#### *Books*

Settles, G.S., "Schlieren and Shadowgraph Techniques," 2001, pp. 30